The Journal of Energy: Engineering & Management
Vol. 2, No. 4, Winter 1391, P. 58-69

Natural Convection at Different Prandtl Numbers in Rectangular Cavities with a Fin on the Cold Wall

S. Jani[1*], M. Mahmoodi[2], M. Amini[3]

[1] Faculty of Engineering (Assistant Professor), Golpayegan College of Engineering, Golpayegan, I.R. Iran
jani@gut.ac.ir

[2] Department of Mechanical Engineering (MSc student) University of Kashan, Kashan, I.R. Iran
mahmoodi.m@hotmail.com

[3] Department of Mechanical Engineering (MSc student) University of Kashan, Kashan, I.R. Iran
meysamini@yahoo.com

Received: 10 September 2011 Revised: 23 September 2011

Accepted: 1 May 2012

Abstract

The natural convection in differentially heated rectangular cavities with a fin attached to the cold wall was investigated numerically. The top and the bottom horizontal walls of the cavities were insulated while their left and the right vertical walls were maintained at a constant temperature T_h and T_c, respectively with $T_h > T_c$. The governing equations written in terms of the primitive variables were solved numerically using the finite volume method while the velocity and pressure fields were coupled using the SIMPLER algorithm. Using the developed code effects of pertinent parameters such as length and location of fin, aspect ratio of the enclosure, Rayleigh number, and Prandtl number on heat transfer and fluid flow in the enclosure were investigated. The results showed that for the cavity filled with water, at high Rayleigh numbers, a longer fin placing at the middle of the right wall has more remarkable effect on the heat transfer inside the cavity. Also, it was observed that at low Rayleigh numbers, the effect of fin on heat transfer enhancement in low Prandtl numbers is more than that in high Prandtl numbers. Moreover, it was found that the fin has more effect for narrow enclosures.

Keywords: Free Convection, Rectangular Cavity, Numerical Simulation, Thin Fin, Prandtl number.

* **Corresponding Author**

1. Introduction

Free convection fluid flow and heat transfer occurs in many industrial and engineering systems such as solar energy collectors, home ventilation systems, energy storage systems, refrigeration unit, fire prevention, etc. [1]. In general, increasing, controlling, and modification of fluid flow and heat transfer inside the differentially heated cavities is down using a partition or fin attached to the walls of the cavity. Many researchers have investigated free convection inside cavities with fin on the walls. Frederick [2] studied numerically laminar free convection in an air filled differentially heated inclined enclosures with a thin partition placed at the middle of its cold wall. Decreasing heat transfer of up to 47 percent in comparison with the cavity with no partition was observed in this study. Frederick and Valencia [3] studied free convection heat transfer in a square cavity with a conducting partition located at the middle of its hot wall using numerical simulation. They observed that for a low value of the partition-to-fluid thermal conductivity ratio and for Rayleigh numbers from 10^4 to 10^5 a reduction in heat transfer relative to the case of cavity with no partition occurs. Scozia and Frederick [4] investigated numerically free convection in a tall cavity with multiple conducting fins on the cold wall. They found that as the inter fin aspect ratio is varied from 20 to 0.25, the flow patterns evolve considerably and the average Nusselt number reaches maximum. Nag et al. [5] investigated the effect of a horizontal thin partition positioned on the hot wall of a horizontal square cavity. They observed that for a partition of infinity thermal conductivity the Nusselt number on the cold wall was greater than the case with no fin. Lakhal et al. [6] studied numerically free convection in rectangular enclosures with perfectly conducting fin attached to the hot wall. Bilgen [7] investigated laminar and turbulent free convection in cavities with partition positioned on the insulated horizontal walls. His study covered various geometrical parameters such as: aspect ratio of cavity, number of partitions, position of partitions, length of partitions, and Rayleigh number. He found that the heat transfer was reduced when two partitions were used instead of one, the aspect ratio was made smaller, and the position of partitions was farther away from the hot wall. Shi and Khodadadi [8] reported results of a numerical study of laminar free convection in a differentially heated square cavity due to a perfectly conducting thin fin on its hot wall. They found that heat transfer on the cold wall without fin can be promoted for high Rayleigh numbers and with the fins placed closer to the insulated walls. Ben-Nakhi and Chamkha [9] investigated effects of length and inclination of a thin fin placed on the middle of hot wall on free convection in a square cavity using numerical simulation. They found that the Rayleigh number, thin fin inclination, and length have significant effects on the average Nusselt number of the heated wall including the fin of the enclosure. Oztop and Bilgen [10] studied free convection in a square cavity differentially heated on vertical walls, insulated on horizontal walls, and with a cold partition on the bottom wall. They found that in the presence of a cold partition the heat transfer reduced and the heat reduction gradually increased with an increase in partition height and thickness .The heat transfer reduced more effectively when the partition is closer to the hot or cold wall. Frederick [11] studied numerically free convection of air in a cubical enclosure with a thick partition fitted vertically on the hot wall. Sheikhzadeh et al. [12] investigated numerically free convection heat transfer inside a differentially heated square cavity with two perfectly conductive thin fins attached to the isothermal walls. They found that when the dimensionless length of the fins is 0.5, and for Rayleigh number from 10^4 to 10^7, the Nusselt number remains constant. Results of a numerical study on free convection in a partially heated square cavity with a thin fin on its hot wall were reported by Ben-Nakhi et al. [13]. They considered a square cavity with hot left wall and a perfectly conductive thin fin on it, insulated horizontal walls, and partially opened on its right wall. Their results showed that fin attachment tended to increase heat transfer at a given Rayleigh number because of the active area added. The problem of natural convection in differentially heated square enclosures with multiple fins on its hot wall under electric field effect was investigated by Kasayapanand [14] numerically. He found that the heat transfer coefficient was substantially improved by the electric field effect especially at high number of fins and long fin length.

Based on the above mentioned articles it was found that to increase the rate of heat transfer inside the differentially heated cavities a high conductive fin on the walls of the cavity can be used. The pertinent parameters in this problem are length and location of the fin. In the present study, the free convection fluid flow and heat transfer in a differentially heated square cavity with a fin attached to its cold wall is simulated numerically using the finite volume method. The left and the right vertical walls are kept at a constant temperature T_h and T_c, respectively. The cavity's top and bottom walls are insulated. The governing equations are solved using the SIMPLER algorithm. A parametric study is performed, and the effects of Rayleigh number, length of fin, position of fin on the right wall of the cavity, Prandtl number, and aspect ratio of cavity on the fluid flow and heat transfer inside the cavity are investigated. This problem occurs when an electronic device is located in a cavity and the heat is removed by the cold wall of the cavity. The thin fin is attached to the cold wall to increase the cold surface which affects the rate of heat transfer of the electronic device. Moreover, in order to control and manage the heat transfer and temperature distribution inside the cavity, the thin fin can be used.

2. Problem definition

A schematic view of the cavity considered in the present study and the coordinate system are shown in Fig. 1. The width and the height of the cavity are denoted by H and W, respectively. The left vertical wall of the cavity is kept at a constant temperature T_h, while its right vertical wall is maintained at temperature T_c with $T_h > T_c$. The top and the bottom horizontal walls are kept insulated. A highly conductive thin fin is attached to the cold wall. The length and the location of the thin fin on the right wall are shown with l and s, respectively. The dimensionless variables $L = l/W$ and $S = s/H$ are defined as the length and location of the thin fin, respectively. The aspect ratio of the cavity is defined as $AR = H/W$. It is assumed that the fin is highly conductive and is maintained at the same temperature of the wall to which it is attached. The fluid inside the cavity is considered to be incompressible, and the two-dimensional flow is assumed to be steady and laminar. The properties of the fluid are assumed to be constant with the exception of the density which varies according to the Boussinesq approximation.

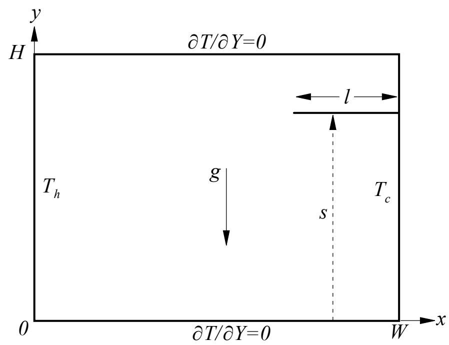

Fig. 1. A schematic view of a square cavity with a thin fin and the boundary conditions

3. Mathematical formulation

In order to express the governing equations in a dimensionless form, the following dimensionless variables are defined:

$$X = \frac{x}{H},\ Y = \frac{y}{H},\ U = \frac{uH}{\alpha},\ V = \frac{vH}{\alpha},$$
$$P = \frac{pH^2}{\rho\alpha^2},\ \theta = \frac{T - T_c}{T_h - T_c}, \tag{1}$$

where $u(U)$ and $v(V)$ are the velocity components in the x-(X-) and y-(Y-) directions, $T(\theta)$ is the temperature, and $p(P)$ is the pressure. Also, α and ρ are the thermal diffusivity and the density, respectively.

Using the above dimensionless variables, the steady-state continuity, momentum, and energy equations for the laminar natural convection inside the cavity in dimensionless form are given by:

$$\frac{\partial U}{\partial X} + \frac{\partial V}{\partial Y} = 0, \tag{2}$$

$$U\frac{\partial U}{\partial X} + V\frac{\partial U}{\partial Y} = -\frac{\partial P}{\partial X} + Pr\left(\frac{\partial^2 U}{\partial X^2} + \frac{\partial^2 U}{\partial Y^2}\right), \tag{3}$$

$$U\frac{\partial V}{\partial X} + V\frac{\partial V}{\partial Y} = -\frac{\partial P}{\partial Y} + Pr\left(\frac{\partial^2 V}{\partial X^2} + \frac{\partial^2 V}{\partial Y^2}\right) + Ra\,Pr\,\theta, \tag{4}$$

$$U\frac{\partial \theta}{\partial X} + V\frac{\partial \theta}{\partial Y} = \frac{\partial^2 \theta}{\partial X^2} + \frac{\partial^2 \theta}{\partial Y^2}, \tag{5}$$

where the Rayleigh number Ra, and the Prandtl number Pr are defined as:

$$Ra = \frac{g\beta\Delta T H^3}{\alpha\upsilon},\ Pr = \frac{\upsilon}{\alpha}, \tag{6}$$

where β and υ are the volumetric expansion coefficient and the kinematic viscosity, respectively. The dimensionless boundary conditions are:

$$\begin{aligned}
&\text{On the right wall} &&: U = V = 0,\ \theta = 0,\\
&\text{On the left wall} &&: U = V = 0,\ \theta = 1,\\
&\text{On the top wall} &&: U = V = 0,\ \partial\theta/\partial Y = 0,\\
&\text{On the bottom wall} &&: U = V = 0,\ \partial\theta/\partial Y = 0,\\
&\text{On the fin} &&: U = V = 0,\ \theta = 0.
\end{aligned} \tag{7}$$

The relation for the local Nusselt number can be written as:

$$Nu_{local} = -\left.\frac{\partial \theta}{\partial X}\right|_{X=0}. \tag{8}$$

The wall-averaged Nusselt number can then be obtained from:

$$Nu = \int_0^1 Nu_{local}\, dY. \tag{9}$$

In addition, a variable called the Nusselt number ratio (NNR), is introduced as follows:

$$NNR = \frac{Nu|_{with\ a\ fin}}{Nu|_{without\ a\ fin}}. \tag{10}$$

4. Numerical approach

The governing equations are discretized using the finite volume method and the coupling between the velocity and pressure fields is done using the SIMPLER algorithm. The diffusion terms in the equations are discretized by a second order central difference scheme, while a hybrid scheme (a combination of the central difference scheme and the upwind scheme) is employed to approximate the convection terms. The set of discretized equations are solved by TDMA line by line method [15]. The computations are carried out for the Rayleigh number between 10^3 and 10^6.

To validate the numerical procedure, the results obtained by the present code for a differentially-heated square cavity filled with air and with a thin fin with different length located at the middle of hot wall, were compared with the results of Shi and Khodadadi [8]. Table 1 shows a comparison for the Nusselt number ratio (*NNR*) of the cold wall of the cavity, which is defined according to (10), obtained by the present work with the results of Shi and Khodadadi at Ra = 10^7. Based on the table, very good agreement exists between the results.

Table 1. Comparison of the present results for the *NNR* of the cold wall with the results of Shi and Khodadadi

	Present study	Shi and Khodadadi [8]
L = 0.20	1.002	1.006
L = 0.35	1.035	1.038
L = 0.50	1.060	1.063

To conduct a grid independence study, the natural convection in a square cavity with length and location of the fin equal to 0.5 and 0.5 respectively and filled with water with Pr = 6.8 at Ra = 10^6 was considered. Five different uniform grids, namely, 21×21, 41×41, 61×61, 81×81, and 101×101 are employed for the numerical calculations. The average Nusselt numbers of the hot vertical wall of the cavity for each of the five grids are presented in Table 2. According to the table, a uniform 81×81 grid is sufficiently fine for the numerical calculation. All the results presented in the following have been obtained by using this grid.

Table 2. Average Nusselt number for different grid sizes

Grid Size	21×21	41×41	61×61	81×81	101×101
Nu	5.961	8.802	10.674	11.031	11.033

5. Results and discussion

Having validated the numerical procedure via solving the test case, the code is employed to investigate the natural convection fluid flow and heat transfer inside the cavity with a fin attached to its cold wall. The results are presented for a range of Ra from 10^3 to 10^6 with a fin at different lengths, L = 0.25, 0.5, and 0.75, three various positions of the fin, S, namely, 0, 0.25, 0.5, and 0.75, the Prandtl number ranging from 0.1 to 10 and the aspect ratio of cavity which varies from 4 to 0.25.

At the first step, a square cavity filled with water with Pr = 6.8 is considered and different positions and lengths of the thin fin are examined to find optimal length and location of the fin.

Figs. 2(a) and 2(b) show the streamlines and the isotherms for a square cavity with a fin at its lower position (S = 0.25), and for various Ra and different lengths of the fin, L = 0.25, 0.5, and 0.75, respectively. The plots are arranged going from left to right with the ascending of the Rayleigh number. For the all values of Ra, a large clockwise (CW) rotating cell is observed for all fin lengths (Fig. 2(a)). The fluid that is heated next to the hot wall (left wall) rises and replaces the cooled fluid next to the cold wall (right wall) that is falling, thus giving rise to a CW rotating vortex (also called the primary vortex). Due to this figure, as the Rayleigh number increases, the flow patterns and the temperature

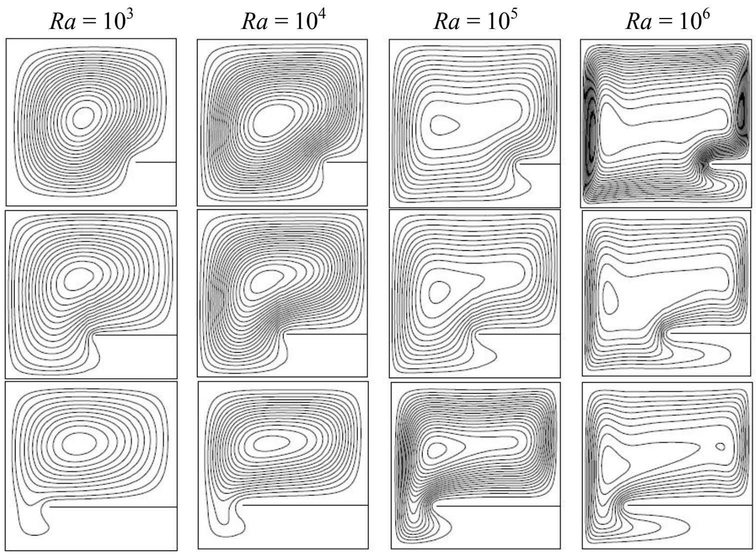

(a)

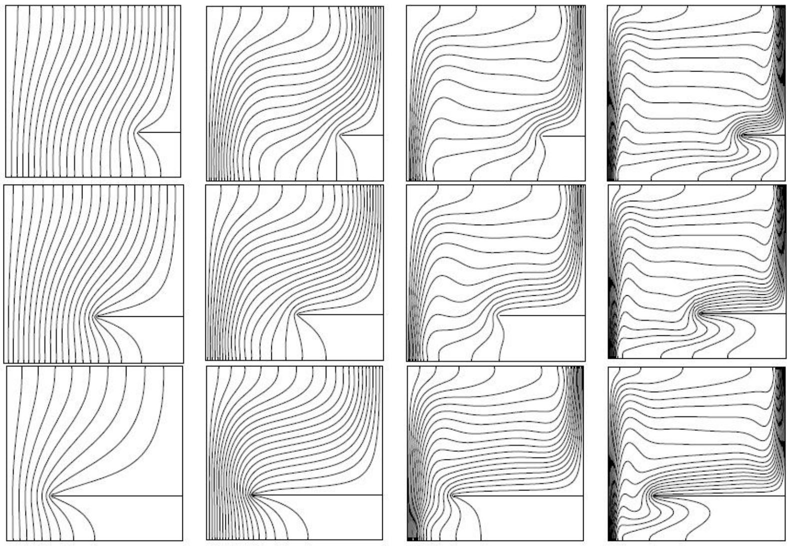

(b)

Fig. 2. Streamlines and isotherms inside the square cavity for various *Ra* and different fin's length for *S* = 0.25; (a) streamlines (b) isotherms

distribution change from the conduction to convection-dominated regime for all the L values. It seems that the various lengths of the fin not only change the flow fields near the fin, but they also relatively change the strength of the CW vortex. This is because the fin blocks the movement of the fluid and weakens the CW vortex.

The flow and the temperature fields in the cavity, due to the streamlines and the isotherms, are presented in Figs. 3(a) and 3(b) for the middle position of a fin (S = 0.5), and Figs. 4(a) and 4(b) for a fin at its upper position (S = 0.25), respectively. Note that the plots are arranged going downward with the ascending of the L value. By increasing the Rayleigh number, similar treatment corresponding to the flow (Figs. 3(a) and 4(a)) and temperature (Figs. 3(b) and 4(b)) distribution can be seen between these figures and those of Figs. 2(a) and 2(b), respectively. By comparing all the cases in Figs. 2(a), 3(a), and 4(a), it is possible to see that a fin attached to the middle of the wall has the most remarkable effect on the fluid flow in the cavity. A fin redirects the movement of the fluid and weakens the fluid motion within the area under the fin for $S < 0.5$, whereas it weakens the fluid motion within the area above the fin while $S \leq 0.5$. In general, the presence and the character of the primary CW rotating vortex is unaltered, with a longer fin bringing about more changes to the flow compared to a shorter fin. For $Ra = 10^4$, the streamlines and the isotherms near the fin exhibit similar trends as those for $Ra = 10^3$, and in some instances, the flow field exhibits two local minima that may be reminded for the common cases of a cavity with no fin. At the moderate Rayleigh numbers ($Ra = 10^5$), the boundary layer regime is developed towards the cavity walls and for higher Ra, the convective mode of heat transfer is dominated throughout the cavity. Moreover, the more packed stream function

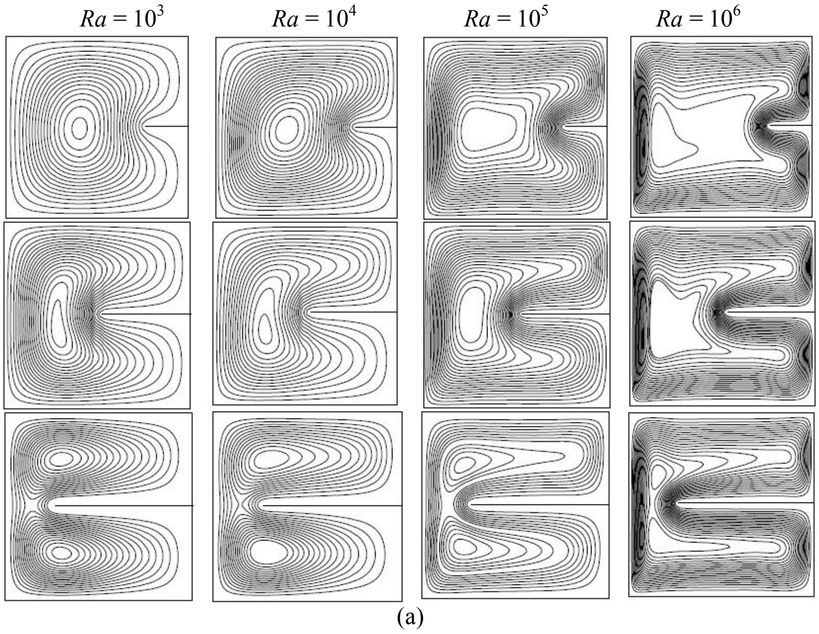

(a)

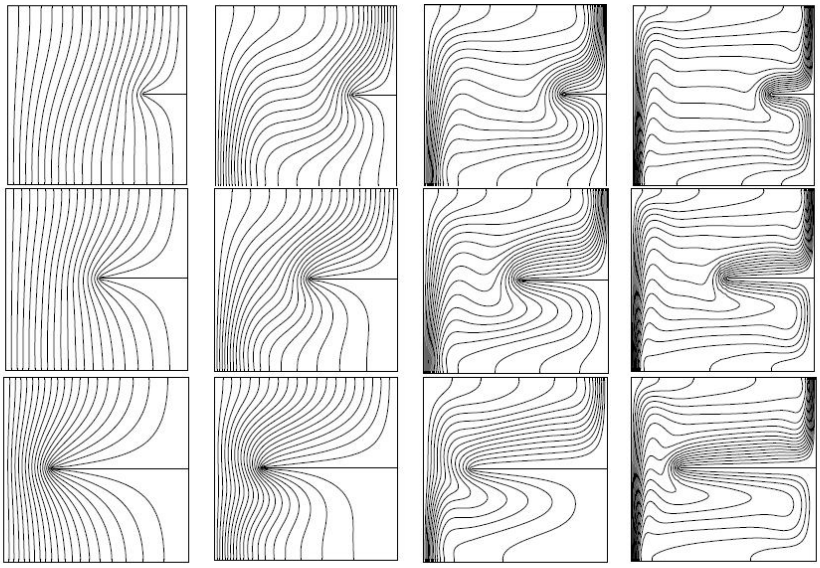

(b)

Fig. 3. Streamlines and isotherms inside the square cavity for various *Ra* and different fin's length for *S* = 0.5; (a) streamlines (b) isotherms

contours indicate that the fluid moves faster as the Rayleigh number increases.

For the case of $Ra = 10^4$ (convection not being strong compared to conduction), presence of the fin brings resistance to the motion of the CW vortex and it has the most remarkable effects on the flow field when it is placed at the middle of the left wall. Also, placing a fin near the right upper corner can enhance the primary vortex somewhat. This is because the fluid moves slowly in this area and a cold fin placed at $S > 0.75$ cools the hot fluid coming toward it from the left wall. For such a situation, a longer fin results in a stronger primary vortex. It is observed that for the case of $Ra = 10^5$ (convection dominating conduction), a fin can block the flow, thus weakening the primary vortex, but at the same time a long enough cold fin can cools the fluid and make it lighter resulting in enhancement of the CW vortex. These two mechanisms are found to certainly counter balance each other for nearly the fin's middle position, regardless of the fin's length. At $Ra = 10^6$, given the strong effect of free convection implies that placing a fin of any length can always enhance the primary vortex regardless of its position. It should be noted that at $Ra = 10^6$ the fin's effect of blocking the fluid motion is more dominant than effect of cooling the fluid to enhance the primary vortex.

In order to compare the temperature fields for all cases, Figs. 2(b), 3(b), and 4(b) are considered again. The value of θ on the right wall and the fin is 0, whereas the value of θ on the left wall is 1. Comparing these figures for $Ra = 10^6$, a fin with $L = 0.25$ at most positions only changes the temperature distribution locally and the rest of the cavity remains unaffected. This is because the CW vortex has not altered too much upon introduction of a 0.2 W long fin and the fin only changes the velocity distribution locally. As mentioned before, a fin at $S < 0.5$ can weaken the fluid motion in the area below the fin and

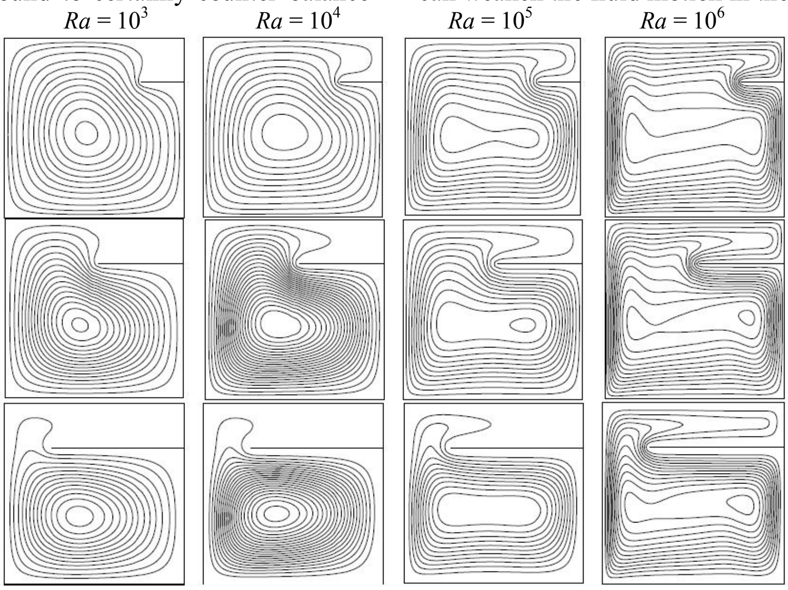

(a)

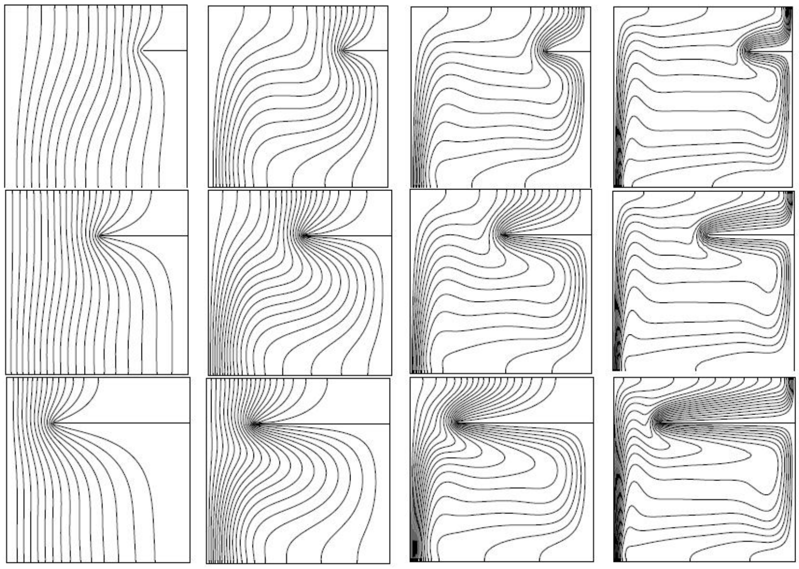

(b)

Fig. 4. Streamlines and isotherms inside the square cavity for various *Ra* and different fin's length for *S* = 0.75; (a) streamlines (b) isotherms

thus decreased heat transfer capability is expected. Moreover, at the higher Rayleigh numbers, the temperature contours above the fin are more packed than those under the fin. This implies better heat transfer on the top surface of the fin than on the bottom surface for almost all mentioned values of *S*. For longer fins, the temperature contours to the left of the fin are affected by the introduction of the fin. Higher temperature gradients next to the left wall are observed while placing a longer fin on the right wall compared to placing a shorter one.

In order to study the effect of the fin on the average heat transfer rate in the cavity, a variable named *NNR* is used which can be obtained according to [8]. Value of *NNR* greater than 1 indicates that the heat transfer rate is enhanced in the cavity, whereas reduction of heat transfer is indicated when *NNR* is less than 1. Thus, the average Nusselt number can be obtained from the product of *NNR* and average Nusselt number for a no-fin cavity in Table 3.

Table 3. Average Nusselt number of the hot wall of the square enclosure with no fin, filled with water with *Pr* = 6.8

Ra	10^3	10^4	10^5	10^6
Nu	1.144	2.314	4.797	9.317

Figures 5(a), 5(b), and 5(c) show the variations of *NNR* with respect to the fin's position for three different lengths of the fin, *L* = 0.25, 0.5, and 0.75 for *Ra* = 10^4 to 10^6, respectively. Based on these figures, it is observed that placing a fin on the right wall always increases the heat transfer in cavity, except that for *Ra* = 10^4, when *L* = 0.5, and $0.25 \leq S \leq 0.5$. For *Ra* = 10^4, the effect of the fin's length on the mean heat transfer is more remarkable for longer fin's lengths, regardless of the fin's position, *S*.

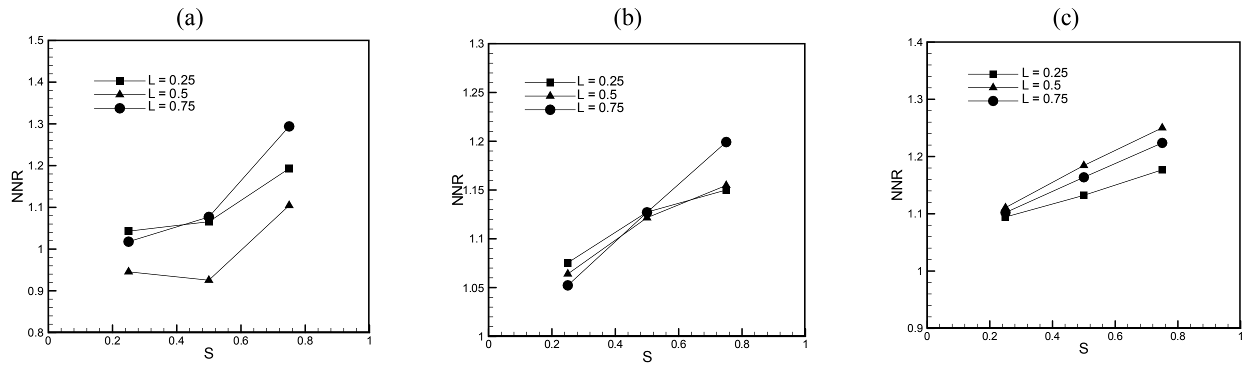

Fig. 5. Variation of the *NNR* along the heated wall of the cavity with respect to position of the fin; (a) *Ra* = 10^4, (b) *Ra* = 10^5 and (c) *Ra* = 10^6

Upon comparing the diagrams of Fig. 5, it is possible to see that the effect of the fin's length on *NNR* becomes less remarkable with the rise of the Rayleigh number due to the fact that these three curves come closer. This is because the effect of the cold fin cooling the flow and enhancing the primary vortex can compensate the effect of the fin blocking the flow. Moreover, it can clearly be seen from Fig. 5(c), that for *Ra* = 10^6, placing a fin at the middle of the right wall has more remarkable effect on the mean Nusselt number compared to placing it on the two ends of the left wall.

In the second step, a square cavity with a thin fin with $L = 0.75$ located in $S = 0.5$ is chosen and effect of Prandtl number on flow pattern, temperature distribution, and heat transfer inside the cavity is investigated.

Fig. 6 and 7 show the streamlines and isotherms inside the cavity with a fin with $L = 0.75$ and located in $S = 0.5$ at different Rayleigh and Reynolds numbers, respectively. As can be seen from the streamlines, at $Ra = 10^4$ for all Prandtl numbers considered an eddy is developed inside the cavity. The central region of this eddy is composed of two secondary vortices which are located under and over the fin. The shape of the secondary eddies are similar for all Prandtl numbers at $Ra = 10^4$. At $Ra = 10^5$ different flow patterns are observed for different Prandtl numbers. At $Pr = 0.1$, the eddy located over the fin is bigger than that located under the fin. By increasing the Prandtl number, while the Rayleigh number is kept at 10^5, the eddy under the fin increases in size. At $Ra = 10^6$ and $Pr = 0.1$ a little eddy is developed under the fin. Moreover at this Rayleigh and Prandtl number, the central region of the primary eddy breaks into two smaller eddies. An increase in Prandtl number, while the Rayleigh number is kept at 10^6, the little eddy under the fin disappears and the streamlines are formed parallel with the fin and horizontal walls.

The isotherms at $Ra = 10^4$ show characteristics of conduction heat transfer for all range of Prandtl number considered. At $Ra = 10^5$ the isotherms are condensed adjacent to the lower left corner of the cavity. An increase in Prandtl number, while the Rayleigh number is kept at 10^5, the isotherms are condensed adjacent to the upper right corner of the cavity. For all Prandtl numbers at this Rayleigh number, thermal stratification is observed in the region over the fin. A similar trend is observed at $Ra = 10^6$.

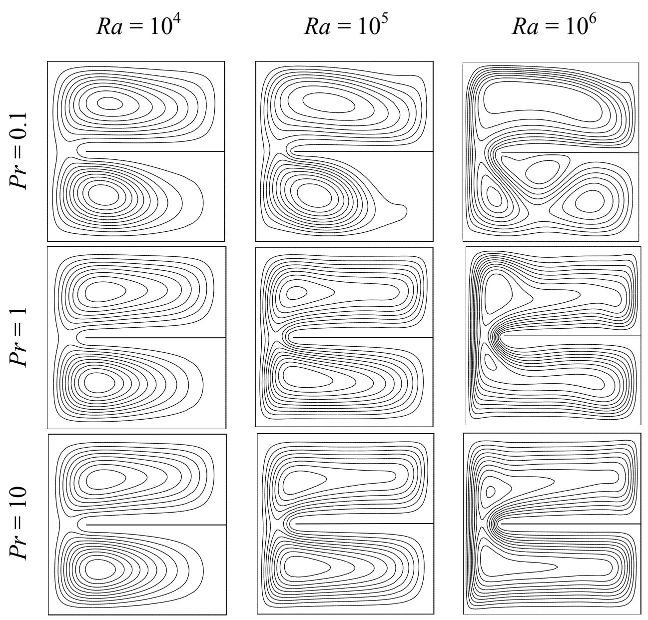

Fig. 6. Streamlines inside the square cavity having a thin fin with $L = 0.75$ and position of $S = 0.5$ for various Pr

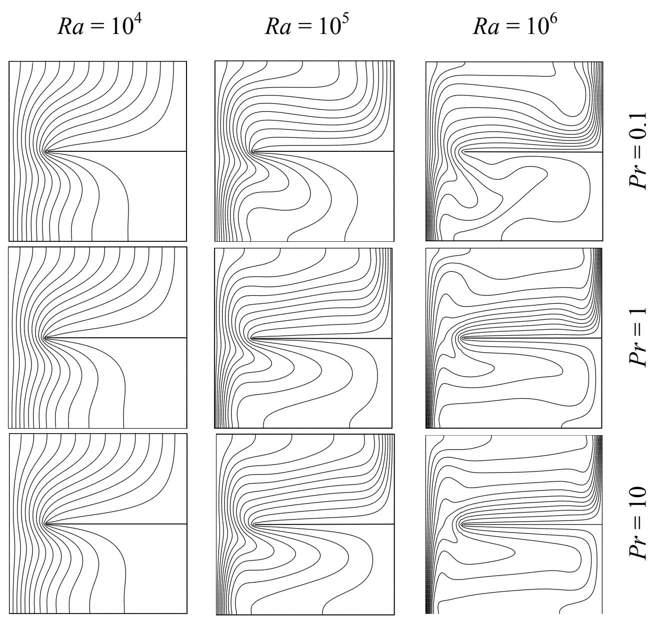

Fig. 7. Isotherms inside the square cavity having a thin fin with $L = 0.75$ and position of $S = 0.5$ for various Pr

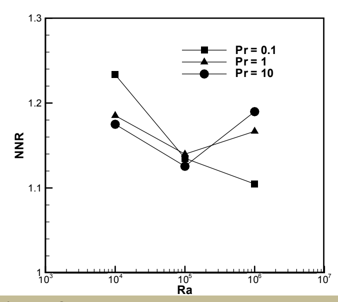

Fig. 8. Variation of *NNR* along the heated wall of the cavity having a fin with $L = 0.75$ and $S = 0.5$ versus Pr

Table 4. Average Nusselt number of the hot wall of the square cavity with no fin at different Prandtl numbers

Ra	10^4	10^5	10^6
$Pr = 0.1$	2.164	3.972	7.358
$Pr = 1$	2.293	4.673	9.069
$Pr = 10$	2.314	4.800	9.321

Fig. 8 shows variation of *NNR* with respect to Rayleigh number for different Prandtl numbers. The average Nusselt number is obtained from the product of *NNR* and average Nusselt number for a no-fin cavity in Table 4.

As can be observed from the figure, at different Rayleigh numbers, effect of fin on enhancement of heat transfer varies. It is evident from the figure that at $Ra = 10^4$ as the Prandtl number decreases, effect of fin on enhancement of heat transfer increases. At $Ra = 10^5$ similar *NNR*s are obtained for all Prandtl numbers considered. At $Ra = 10^6$ the effect of fin on enhancement of heat transfer increases with an increase in Prandtl number. As depicted in Fig. 7, at $Ra = 10^6$ as Prandtl number increases, the isotherms over the fin, especially at the left end of the fin, become more condensed which is characteristics of higher effect of fin on enhancements of heat transfer

In the third section, effect of aspect ratio of the finned cavity ($AR = H/W$) on characteristics of heat transfer inside it, is studied. Five different cavities with aspect ratios of 4, 2, 1, 0.5, and 0.25, containing a fluid with $Pr = 1$ having a fin with $L = 0.75$ attached to $S = 0.75$ are considered.

Streamlines and isotherms for the cavity with $AR = 4$ for different Rayleigh numbers are shown in Fig. 9. It is evident from the figure that for all Rayleigh numbers considered, two eddies are developed inside the enclosure which with an increase in Rayleigh number, the eddy located over the fin becomes weaker than that located under the fin. From the isotherms, a conduction dominant heat transfer is observed at $Ra = 10^4$ and 10^5. At $Ra = 10^6$ thermal boundary layers are formed adjacent to the vertical walls and thermal stratification occurs in the region over the fin.

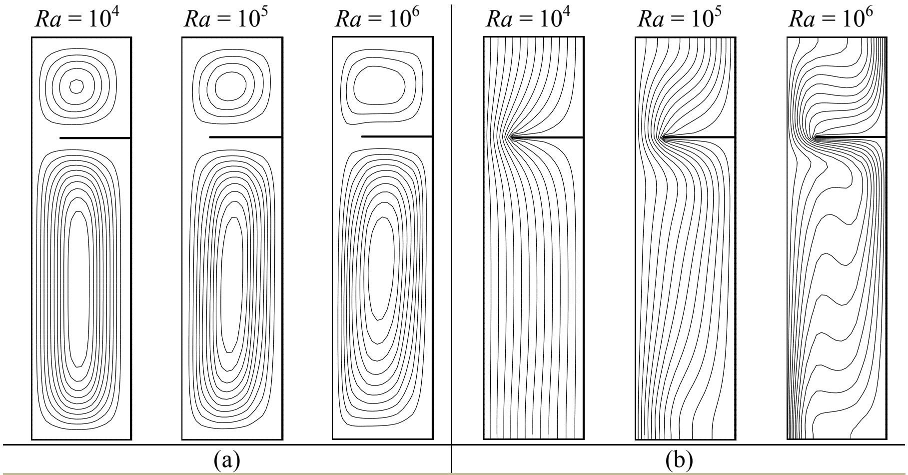

Fig. 9. Streamlines and isotherms inside the rectangular cavity with $AR = 4$ having a fin with $L = 0.75$ and $S = 0.75$ for $Pr = 1$ and various Ra; (a) streamlines (b) isotherms

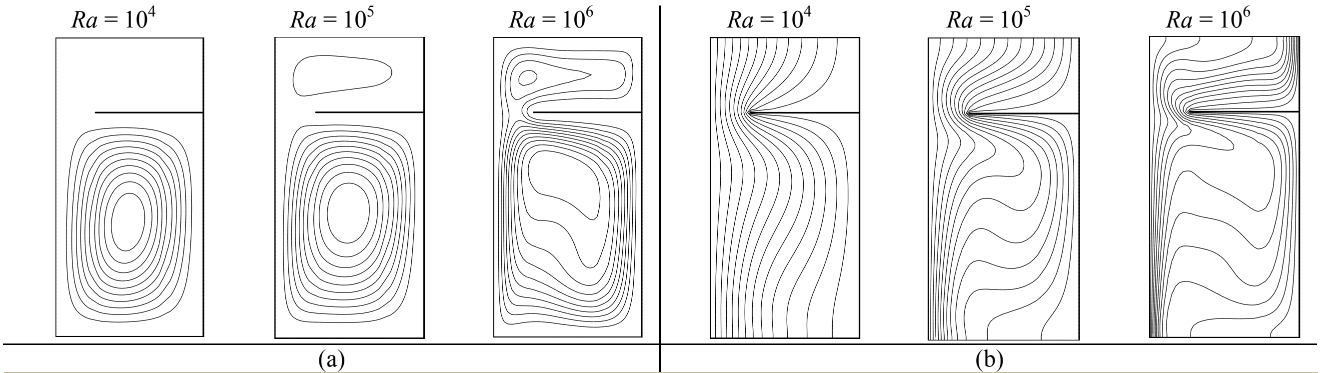

Fig. 10. Streamlines and isotherms inside the rectangular cavity with $AR = 2$ having a fin with $L = 0.75$ and $S = 0.75$ for $Pr = 1$ and various Ra; (a) streamlines (b) isotherms

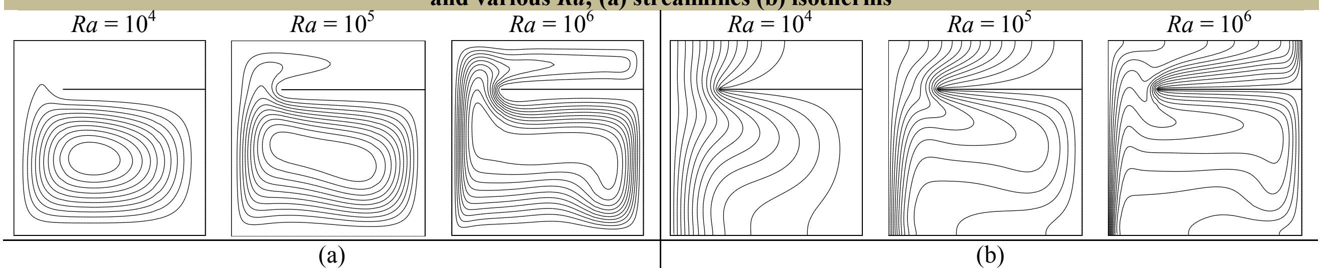

Fig. 11. Streamlines and isotherms inside the rectangular cavity with $AR = 1$ having a fin with $L = 0.75$ and $S = 0.75$ for $Pr = 1$ and various Ra; (a) streamlines (b) isotherms

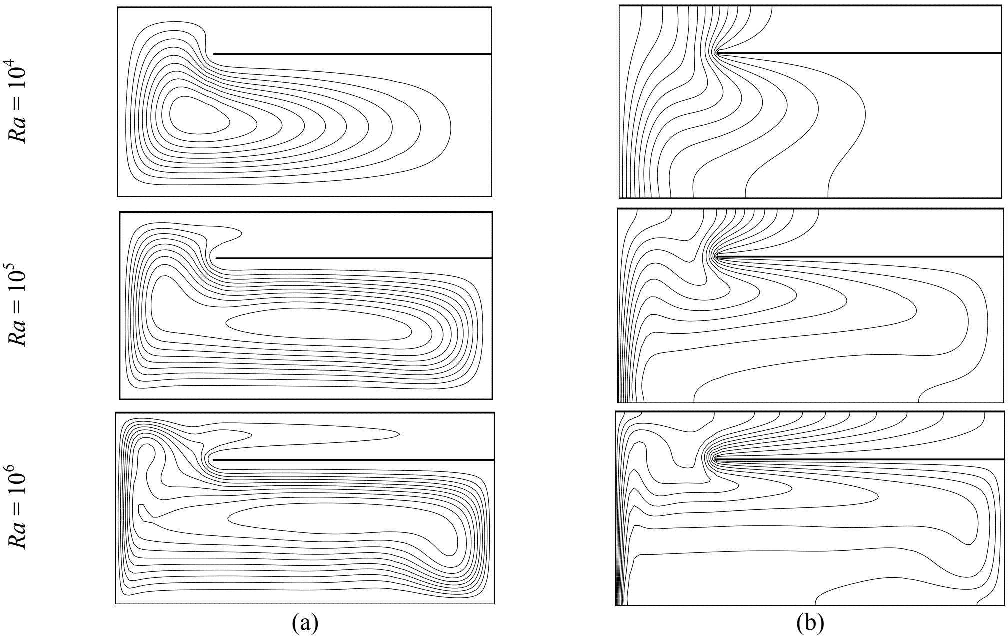

Fig. 12. Streamlines and isotherms inside the rectangular cavity with *AR* = 0.5 having a fin with *L* = 0.75 and *S* = 0.75 for *Pr* = 1 and various *Ra*; (a) streamlines (b) isotherms

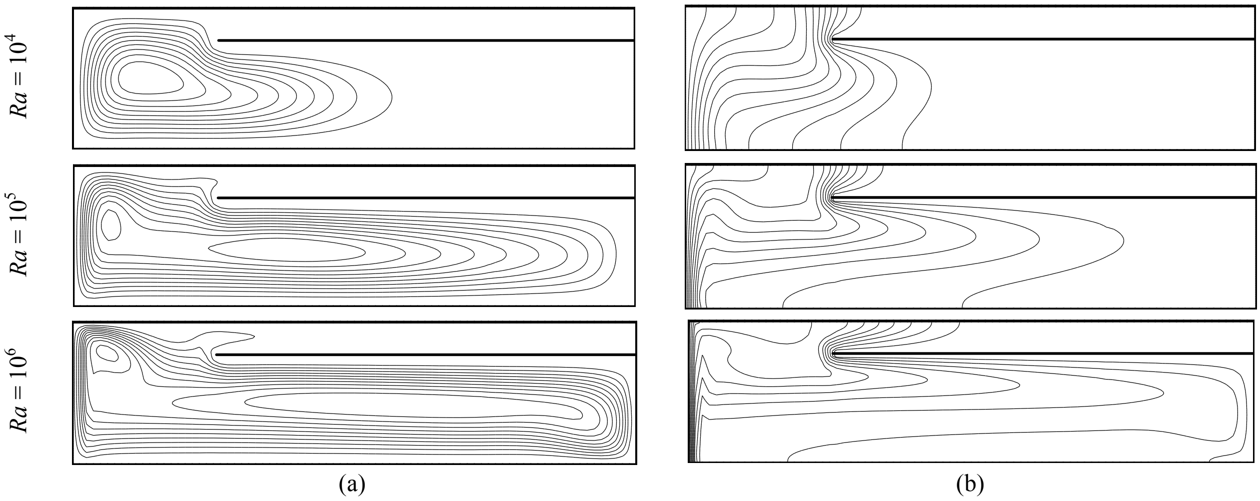

Fig. 13. Streamlines and isotherms inside the rectangular cavity with *AR* = 0.25 having a fin with *L* = 0.75 and *S* = 0.75 for *Pr* = 1 and various *Ra*; (a) streamlines (b) isotherms

Variations of streamlines and isotherms inside the cavity with AR = 2 versus Rayleigh number are shown in Fig. 10. It is observed that at $Ra = 10^4$ a clockwise eddy is formed under the fin and the fluid existing over the fin, is relatively stagnant. By increasing the buoyancy force at $Ra = 10^5$, a weak eddy is developed over the fin. Further increase in buoyancy force at $Ra = 10^6$ the strength of the eddy under the fin increases and it penetrates over the fin. Based on the isotherms it is evident that at $Ra = 10^4$ the heat transfer occurs mainly through conduction while with further increase in the Rayleigh number, the isotherms become more condensed adjacent to the vertical walls which is the characteristics of the natural convection.

Fig. 11 shows streamlines and isotherms inside the cavity with AR = 1 at different Rayleigh numbers. Similar to the results of the cavity with AR = 2, at $Ra = 10^4$ the fluid over the fin is relatively stagnant and there is only an eddy under the fin. By increasing Rayleigh number, this eddy becomes stronger and penetrates over the fin. The mentioned observations about the isotherms of the cavity with AR = 2 are valid here.

The streamlines and isotherms inside the cavities with AR = 0.5 and 0.25, at different Rayleigh numbers are shown in Figs. 12 and 13, respectively. As can be seen from the figures for two cavities with different aspect ratios, at $Ra = 10^4$ a clock wise eddy is developed under the fin. By increasing Rayleigh number the eddy penetrates over the fin and its central region is elongated horizontally. Conduction dominant heat transfer at $Ra = 10^4$ and formation of thermal boundary layers adjacent to the vertical walls at high Rayleigh numbers, is observed from the isotherms in Figs. 12 and 13.

Variations of *NNR* with respect to Rayleigh number for different Prandtl numbers are shown in Fig. 14. The average Nusselt number is obtained from the product of *NNR* and average Nusselt number for a no-fin cavity in Table 5. According to the figure, as the cavity becomes narrower, the effect of fin on enhancement of heat transfer increases.

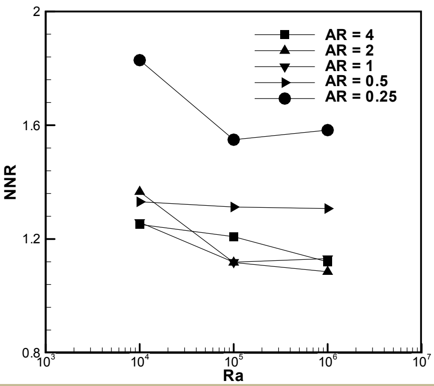

Fig. 14. Variation of *NNR* along the heated wall of the cavity having a fin with *L* = 0.75 and *S* = 0.75 versus *AR*

Table 5. Average Nusselt number of the hot wall of the rectangular cavities with different aspect ratios with no fin, filled with a fluid with *Pr* = 1.

Ra	10^4	10^5	10^6
AR = 4	4.065	5.115	9.835
AR = 2	2.563	4.971	9.358
AR = 1	2.293	4.673	9.067
AR = 0.5	1.761	4.175	8.247
AR = 0.25	1.130	3.450	6.668

6. Conclusions

Using the finite volume method, the natural convection fluid flow and heat transfer in a square cavity with a fin attached to its cold wall was studied numerically. The numerical procedure was validated by comparing the average Nusselt number for a differentially-heated square cavity filled with air obtained by the code with the existing results in the literature. Very good agreements were observed between them. Subsequently, a parametric study was performed and the effects of the Rayleigh number, length of the fin, and its position on the flow pattern and heat transfer were investigated. It was observed that, placing an isothermal horizontal fin on the right cold wall of a differentially heated cavity generally modifies the clockwise rotating primary vortex that is established due to natural convection. The effect of the cold fin cooling the flow and enhancing the primary vortex becomes more marked by the rise of the Rayleigh number. Moreover, placing a longer fin at the middle of the right wall has more remarkable effect on the heat transfer inside the cavity compared to placing it on the two ends of the right wall, especially for the higher values of the Rayleigh number.
From the results of the cavities containing fluids with different Prandtl number, it is observed that when the Prandtl number of the fluid inside the cavity decreases, the effect of fin on enhancement of heat transfer will increase.
Also, the results showed that effect of the fin on increasing the heat transfer for shallow cavities is more than tall cavities.

References

[1] Ostrach, S., "*Natural Convection in Enclosures*", ASME Journal of Heat Transfer, Vol. 110, pp. 1175–1190, 1988.

[2] Frederick, R.L., "*Natural Convection in an Inclined Square Enclosure with a Partition Attached to Its Cold Wall*", International Journal of Heat and Mass Transfer, Vol. 32, pp. 87–94, 1989.

[3] Frederick, R.L., Valencia, A., "*Heat Transfer in a Square Cavity with a Conducting Partition on Its Hot Wall*", International Communication of Heat and Mass Transfer, Vol. 16, pp. 347–354, 1989.

[4] Scozia, R., Frederick, R.L., "*Natural Convection in Slender Cavities with Multiple Fins Attached on an Active Wall*", Numerical Heat Transfer, Part A, Vol. 20, pp. 127–158, 1991.

[5] Nag, A., Sarkar, A., Sastri, V.M.K., "*Natural Convection in a Differentially Heated Square Cavity with a Horizontal Partition Plate on the Hot Wall*", Computer Methods in Applied Mechanics and Engineering, Vol. 110, pp. 143–156, 1993.

[6] Lakhal, E.K., Hasnaousi, M., Bilgen, E., Vasseur, P., "*Natural Convection in Inclined Rectangular Enclosures with Perfectly Conducting Fins Attached on the Heated Wall*", Heat and Mass Transfer, Vol. 32, pp. 365–373, 1997.

[7] Bilgen, E., "*Natural Convection in Enclosures with Partial Partitions*", Renewable Energy, Vol. 26, pp. 257–270, 2002.

[8] Shi, X., Khodadadi, J.M., "*Laminar Natural Convection Heat Transfer in a Differentially Heated Square Cavity Due to a Thin Fin on the Hot Wall*", ASME Journal of Heat Transfer, Vol. 125, pp. 624–634, 2003.

[9] Ben-Nakhi, A., Chamkha, A.J., "*Effect of Length and Inclination of a Thin Fin on Natural Convection in a Square Enclosure*", Numerical Heat Transfer, Part A, Vol. 50, pp. 381–399, 2006.

[10] Oztop, H., Bilgen, E., "*Natural Convection in Differentially Heated and Partially Divided Square Cavities with Internal Heat Generation*", International Journal of Heat Fluid Flow, Vol. 27, pp. 466–475, 2006.

[11] Frederick, R.L., "*Heat Transfer Enhancement in Cubical Enclosures with Vertical Fins*", Applied Thermal Engineering, Vol. 27, pp.1585–1592, 2007.

[12] Sheikhzadeh, Gh.A., Pirmohammadi, M., Ghassemi, M., "*A Numerical Study of Natural Convection in a Cavity with Two Fins Attached to Its Vertical Walls*", ASME International Mechanical Engineering Congress and Exposition, November 11-15, Seattle, Washington, USA, 2007.

[13] Ben-Nakhi, A., Eftekhari, M.M., Loveday, D.I., "*Natural Convection Heat Transfer in a Partially Open Square Cavity with a Thin Fin Attached to the Hot Wall*", ASME Journal of Heat Transfer, Vol. 130, pp. 1–9, 2008.

[14] Kasayapanand, N., "*A Computational Fluid Dynamics Modeling of Natural Convection in Finned Enclosure Under Electric Field*", Applied Thermal Engineering, Vol. 29, pp. 131–141, 2009.

[15] Patankar, S.V., "*Numerical Heat Transfer and Fluid Flow*", Hemisphere Publishing Corporation, Taylor and Francis Group, New York, 1980.